Progress In Electromagnetics Research, PIER 103, 1–16, 2010

MAGNETIC INTERACTION BETWEEN TWO NON-MAGNETIC PARTICLES MIGRATING IN A CONDUCTIVE FLUID INDUCED BY A STRONG MAGNETIC FIELD — AN ANALYTICAL APPROACH

Z. Sun, M. Guo, F. Verhaeghe, J. Vleugels, O. Van der Biest and B. Blanpain

Department of Metallurgy and Materials Engineering
Katholieke Universiteit Leuven
Kasteelpark Arenberg 44, BE-3001 Heverlee (Leuven), Belgium

Abstract—An analytical approach is developed in the present paper to investigate the interaction between two non-magnetic particles migrating in a conductive fluid due to an imposed strong magnetic field (e.g., 10 Tesla). The interaction between the conductive fluid and a single particle migrating along the magnetic lines is influenced by the magnetic field and can be represented by an additional fluid viscosity. Thus the effective fluid viscosity is discussed and the magnetic field effect on the particle migrating velocity is examined. For two particles, two kinds of magnetic forces are induced: namely, the attractive force due to the magnetisation and the repulsive force caused by the conductive fluid flow around the non-magnetic particles. The forces are then evaluated with the consideration of the magnetic field effect on the particle migration and become significant with the increase of the magnetic flux density. The counteracting behavior with a critical particle size of the interparticle magnetic forces is discussed and compared with different magnetic field densities and gradient values.

1. INTRODUCTION

Magnetic interaction is a very important phenomenon governing the behavior of materials in a magnetic field. It has been widely recognised in various research fields, such as magnetic field alignment [1–4], nanocrystals manipulation [5] and particle separation [6]. In earlier reports, most are related with ferromagnetic or super-paramagnetic

Corresponding author: Z. Sun (zhisun@126.com).

materials or with the aid of an additional electrical field [2]. For non-magnetic particles, the interaction forces are very weak under ordinary fields, e.g., $< 1\,\mathrm{T}$, and thus have normally been neglected. However, when the magnetic fields are strong enough, e.g., 10 T, the magnetic interaction forces become significant and the distribution of non-magnetic particles in a bulk material can therefore be controlled only using the magnetic field [7]. As well, distinct phenomena can be observed. For instance, the agglomeration of large non-magnetic particles (e.g., several tens of μm) is restricted in a gradient magnetic field with a magnetic field of 10 T, resulting in finer primary crystal sizes in the metal matrix [8–10] or peculiar particle alignments [7]. The phenomena become more obvious in stronger magnetic fields [7, 10].

In a strong magnetic field of around 10 T, both magnetic and non-magnetic particles, even in sub-micrometer size, in a conductive liquid can be aligned to a magnetically preferred orientation [11–13]. Their assembly morphologies reveal non-negligible interactions between the particles or the growing grains [12]. When the magnetic field exhibits a high gradient, the particles are migrating in the conductive liquid concurrently with their assembling and a local magnetic dipole would be generated with cutting of the magnetic field lines by the pushed liquid in front of each particle [14, 15]. An interparticle interaction due to the conductive fluid flow occurs in parallel with the magnetic dipole-dipole attractive force along the magnetic field direction. Some experimental results have already indicated the presence of this force [10]. However, the magnetic interaction forces are usually in very small magnitudes which make experimental validation difficult.

In such cases, mathematical modeling and analytical calculation can offer a complementary solution for the interpretation and provide direct or intuitional descriptions. Meanwhile, two dimensional analytical calculations have been considered as a very useful tool during magnet design and magnetic field processing [16]. Information such as magnetic field distribution, interaction between the field and materials can be easily obtained [16, 17]. For interparticle magnetic forces, the magnetic dipole-dipole attractive force has been well understood and measured under different conditions both analytically and experimentally by means of ferromagnetic materials [18, 19]. However, limited work has been carried out on the interparticle force due to a conductive melt flow [11, 12]. Therefore, an analytical model was proposed in our previous work [14].

Here a follow-up of our previous research is presented [14, 15]. In this study, an analytical calculation is carried out to describe the non-magnetic particle-particle interaction behaviors in a conductive fluid induced by a strong magnetic field with a high magnetic field gradient.

A specific case of alumina particles migrating in an aluminum melt is considered. Two kinds of interparticle forces, namely, the attractive force due to the magnetisation and the repulsive force caused by the fluid flow around the alumina particles are considered. To perform the calculation, the interaction of the conductive fluid and a single particle migrating along the magnetic lines is evaluated which is represented by and additional fluid viscosity. At the same time, the influence of magnetic fields on the conductive melt viscosity which will directly influence the melt velocity field around the particles is firstly discussed. Subsequently, the cases of different magnetic field densities as well as different magnetic field gradients are investigated to examine the magnetic interaction behaviors between two non-magnetic alumina particles. Based on the calculations, we offer a better explanation of the experimental observations and provide a method for controlling the non-magnetic particles via strong magnetic fields during materials preparation.

2. THEORETICAL BASIS AND CALCULATION DOMAIN

With the development of superconducting technologies, a strong magnetic field of 14 T or more becomes more readily attainable. A vertical strong (z-direction) magnet up to 14 T with a bore size of 150 mm is chosen during the present calculation. The magnetic field intensity as well as the field gradient can be adjusted by changing the current in the superconducting coils. In the magnet, it includes three distinct areas with homogeneous and gradient magnetic fields. In the center of the magnet where $r = 0$ and $z = 0$, the magnetic field intensity has the maximum value and the gradient is zero (homogeneous area). At $z = 0.2$ m, the magnetic field gradient product (BdB/dz) has the largest value and in the range from $z = 0$ to $z = 0.2$ m a diamagnetic material will be pushed to lower magnetic field area which is consistent with the gravity force direction. Figure 1 gives the magnetic field distribution along z-direction when the central magnetic field intensity is 14 T.

2.1. Effect of the Strong Magnetic Field on the Particle Migration

A single Al_2O_3 particle in Al melt undergoes the Faraday force, gravity force, buoyancy force and the viscosity drag force. In most cases, the migration velocity is rather low and the viscosity drag force can be obtained via Stokes' law [25]. According to Fig. 1, the resultant force

F_{res} for one particle in the range from $z = 0$ to $z = 0.2\,\mathrm{m}$ (in the range the Faraday force and the gravity force of a diamagnetic particle are in the same direction) can be expressed as

$$F_{res} = F_P - F_{\eta,B} = \Delta F_m + \Delta G - F_{add} - F_{\eta,B} \tag{1}$$

where F_P is the driving force and ΔF_m is the resultant Faraday force on the non-magnetic particle, ΔG is the difference between gravity force and buoyancy force, F_{add} is the added mass force and $F_{\eta,\mathrm{B}}$ is the Stokes viscosity drag force (B notates for the magnetic field density).

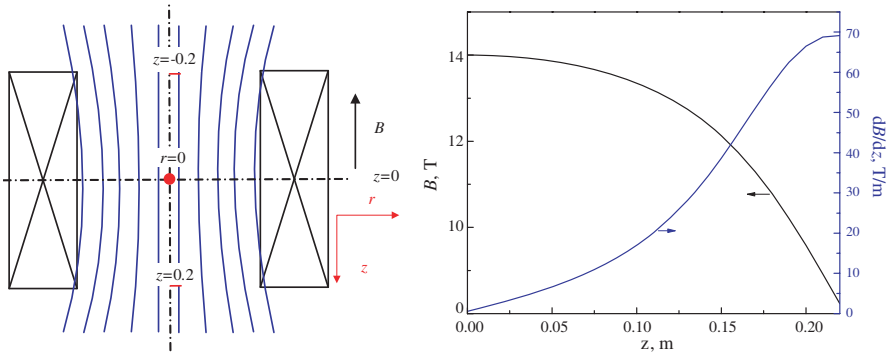

Figure 1. Magnetic field distribution of the chosen superconducting magnet (the blue arrow and the black arrow in the right figure point at the related coordinate axis).

Figure 2 gives a schematic indication of the force analysis of a non-magnetic particle migrating in a conductive fluid. The single contributions in Equation (1) are defined as

$$\Delta G = V(\rho_P - \rho_M)g \tag{2}$$

where ρ_M and ρ_P are the densities of the liquid melt and of the alumina particle, respectively, g is the gravitational constant, V is the volume of the particle.

$$\Delta F_m = V(\chi_M - \chi_P)\frac{1}{\mu_0}B\nabla B \tag{3}$$

where $\mu_0\,(= 4\pi \times 10^{-7}\,\mathrm{Hm^{-1}})$ is the magnetic permeability of vacuum, χ_M and χ_P are, respectively, the volumetric mass magnetic susceptibility of the liquid melt and the diamagnetic particle.

$$F_{add} = \frac{1}{2}\frac{1}{6}\pi d_P^3 \rho_M \frac{dv_P}{dt} \tag{4}$$

where v_P is the particle velocity and t is the time.

For a spherical particle with Reynolds number less than 1, the Stokes drag force is

$$F_{\eta,B} = 3\pi\eta_{M,B}v_P d_P \tag{5}$$

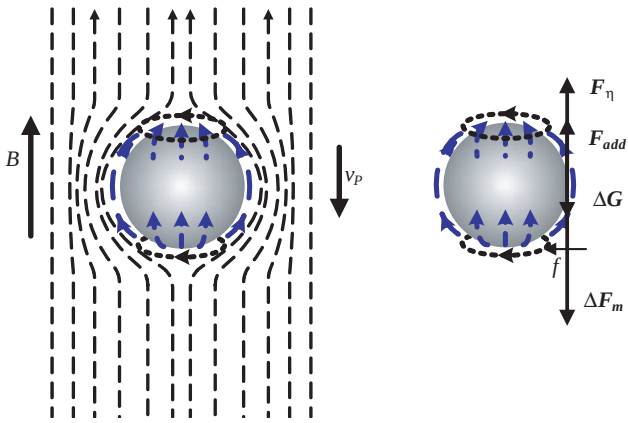

Figure 2. Schematic plot of the force analysis of a non-magnetic particle migrating in a conductive fluid (the blue arrows indicate the fluid direction, the black dashed circle with and an arrow indicates the induced current by the fluid and f is the direction of the induced Lorentz force).

where $\eta_{M,B}$ is the viscosity of the melt under a magnetic field and d_p is the diameter.

A detailed description of the force analysis can be found in [26]. By substituting Equations (2) to (5) into Equation (1), the migration velocities of a non-magnetic particle can be obtained via the following equation according to Newton's second law

$$\left(\rho_P + \frac{1}{2}\rho_M\right)\frac{1}{6}\pi d_P^3\frac{dv_P}{dt} = \frac{1}{6}\pi d_P^3(\chi_M - \chi_P)\frac{1}{\mu_0}B\frac{dB}{dz} + \frac{1}{6}\pi d_P^3(\rho_P - \rho_M)g - 3\pi\eta_{M,B}v_P d_P \quad (6)$$

2.2. Effect of the Strong Magnetic Field on the Particle-particle Interaction

According to [14], the interaction forces of two equal Al_2O_3 particles with a head-to-tail orientation (Fig. 3) along the magnetic field direction (indicating particles migrating one after another along the magnetic field direction) can be investigated after attaining the particle migration velocities.

In a strong magnetic field, the potential energy ($U_{12}^{(m)}$) of the dipole-dipole interaction between particles 1 and 2 can be expressed

as [19]

$$U_{12}^{(m)} = \frac{\mu_0(1+\chi_M)}{4\pi l_{1-2}^3}\left[(\mathbf{m}_1\cdot\mathbf{m}_2) - 3\left(\mathbf{m}_1\cdot\mathbf{e}_{12}\right)\left(\mathbf{m}_2\cdot\mathbf{e}_{12}\right)\right] \quad (7)$$

where $\mathbf{m}_1$, $\mathbf{m}_2$ are the magnetic dipoles, l_{1-2} is the dipole-dipole distance (the particle center is the dipole center) and $\mathbf{e}_{12}$ is the unit vector parallel to the line joining the centers of the two dipoles.

Therefore, the interaction force due to the magnetisation between two equal particles can be caculated by

$$F_{12} = \nabla U_{12}^{(m)} = -\frac{3\mu_0(1+\chi_M)}{4\pi l_{1-2}^4}\left[(\mathbf{m}_1\cdot\mathbf{m}_2) - 3\left(\mathbf{m}_1\cdot\mathbf{e}_{12}\right)\left(\mathbf{m}_2\cdot\mathbf{e}_{12}\right)\right] \left(l_{1-2} \geq \frac{d_1}{2} + \frac{d_2}{2}\right) \quad (8)$$

where the particle size $d_1 = d_2 = d_P$ when the two particles are attached (the separation in Fig. 2 is zero), $\mathbf{m}_1$ and $\mathbf{m}_2$ are the magnetic dipole moments of two magnetised particles and l_{1-2} is the distance between the dipole centers of the two particles (the distance can not be smaller than $d_1/2 + d_2/2$).

As stated in [14], a magnetic dipole is generated at each hemisphere (Fig. 3) when the local melt flow around the particle cuts the magnetic lines. As shown in Fig. 2, four dipoles are induced for two interacting particles. The particle-particle interaction due to the melt flow is derived from the corresponding induced dipoles. The induced dipole moments m' can be calculated if we consider the magnetic dipoles to be point-like according the method in [14].

$$m' = \frac{1}{16}\frac{\pi^3 d_P^4 v_P B \sigma_M}{\ln(\frac{d_P+2\delta}{d_P})} \quad (9)$$

where $\delta = d_P/\sqrt{Re} = d_P/\sqrt{2\rho_M v_P r_P/\eta_{M,B}}$ is the estimated thickness of the liquid aluminum involved [14].

Hence, the interparticle force induced by the aluminum melt flowing around the particle can be derived as

$$F' \cong \frac{3\pi^5\mu_0}{512}\left(-\frac{1}{l_{12}^4} - \frac{1}{l_{34}^4} + \frac{1}{l_{14}^4} + \frac{1}{l_{23}^4}\right)\left[\frac{1}{\ln\left(\frac{d_P+2\delta}{d_P}\right)}\right]^2 d_P^8 B^2 \sigma_M^2 v_P^2 \quad (10)$$

where l_{12}, l_{34}, l_{14} and l_{23} are the induced dipole-dipole distances (Fig. 3).

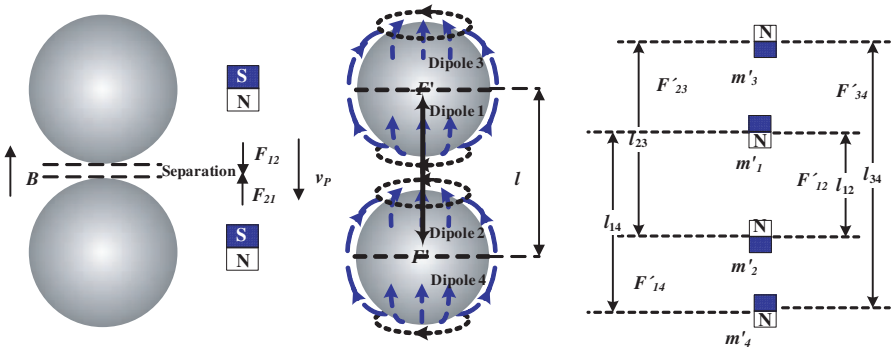

Figure 3. Principles of the magnetic interactions between two particles (the blue arrows indicate the flowing direction around particles; the dashed arrows indicate the induced current direction; the induced dipoles are denoted as m'_1, m'_2, m'_3, m'_4; l_{12}, l_{34}, l_{14} and l_{23} are the distances between the dipoles [14]).

3. RESULTS AND DISCUSSION

A specific case of spherical Al_2O_3 particles migrating in a liquid aluminum with small Reynolds number (laminar flow) is considered in the present investigation and the properties can be found in the related reference books [20, 21]. The densities of Al_2O_3 and liquid aluminum at 933 K are 3970 kg/m^3 and 2370 kg/m^3 respectively. The viscosity η_M of the liquid aluminum at the considered temperature is 1.25×10^{-3} Pa $\cdot$ s [20]. The magnetic susceptibilities of Al_2O_3 and liquid aluminum at 933 K are -1.81×10^{-5} and 1.323×10^{-5} (SI unit) [21]. The electrical conductivity of liquid aluminum at 933 K is $4.132\times10^6(\Omega\cdot\mathrm{m})^{-1}$ [21].

In laminar flow, when two particles are too close to each other or attached, their boundary layers would overlap and make the conditions more complex. To simplify the calculation, we ignored the interaction between the boundary layers. When the separation between two particles is zero (Fig. 3, estimated), the dipole-dipole distance $l = d_P$ and the induced dipole-dipole distances l_{12}, l_{34}, l_{14}, l_{23} can be calculated via the method described in [14] with the results of $l_{12} = 7d_P/15$, $l_{34} = 23d_P/15$ and $l_{14} = l_{23} = d_P$. Therefore, the interaction force F_{12} due to the magnetisation and the force F' due to the fluid flow can be obtained by solving Equations (8) and (9), respectively.

3.1. Effect of the Magnetic Field on the Melt Viscosity

Viscosity is an important physical property that describes the resistance of a deformed fluid and also indicates the nature of the molecules interaction. When a particle is migrating in a liquid melt, the viscosity performs as a drag on the particle and its value depends on the present conditions, e.g., temperature, pressure. After imposing a magnetic field, the interaction behavior and thermodynamics status of the molecules in the liquid melt will be changed and therefore the viscosity of the liquid melt is expected to be modified [22]. Experimental results [23, 24] have demonstrated that the magnetic field can increase the viscosity and some experiential equations have already been derived from the measured data describing the magnetic field dependence of the viscosity [23], e.g., $\eta_{M,B} = \eta_M + AB^2$, where A is a positive constant. However, the mechanisms of how the magnetic field changes the viscosity are still unclear and the previous equation can only fit a single specific case. According to earlier research [10], the increase of the melt viscosity by the applied magnetic field can be due to the induced restriction force when the particle is moving in the melt. As represented in Fig. 4, an additional Lorentz force is induced which would inhibit the particle migration when the particle is moving along or opposite to the magnetic field direction. However, the force is zero when the particle is moving perpendicularly to the magnetic field and thus, the migration can not be influenced. It means the increase of the viscosity only occurs in some specific cases. Therefore, in the case of a particle migrating in a conductive fluid, the increase of the melt viscosity by the applied static magnetic field is

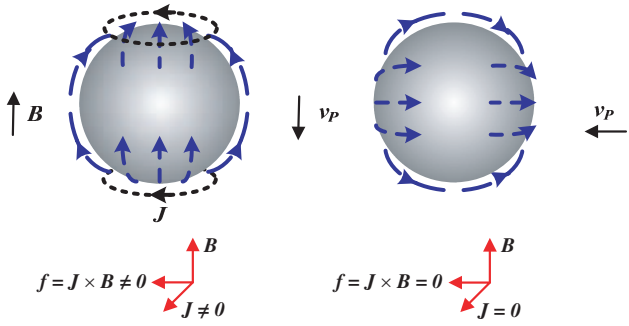

Figure 4. Schematic representation of a particle migration influenced by a magnetic field (the blue arrows indicate the flowing direction of the conductive fluid and the dashed arrows indicate the induced current direction).

more of a representation of the interaction between the particle and the surrounding fluid influenced by the magnetic field. Much more detailed investigations are necessary to obtain a clearer understanding of the magnetic effect on the melt viscosity. However, it is beyond the scope of this paper. Here we will only focus on the previous case when the migration is parallel to the magnetic lines.

When a non-conductive particle is settling along the magnetic lines in a liquid melt under a strong magnetic field, the additional local Lorentz force on the flowing liquid melt is induced by the local liquid melt flow during the migration of the particle which would cut the magnetic field lines and induce some current (Figs. 2 and 4). The local Lorentz force acts as a pressure on the bottom surface of the settling particle, resulting in a contribution to the viscosity drag force [8, 14]. Therefore, the melt viscosity gets a new expression associated with the magnetic field. To represent the additional drag force, analytical method was involved to link the Hartmann number (Ha) to the drag force of the liquid melt on the particle [8, 25]. According to the literatures [8, 25], the drag force D_M can be expressed when $Ha \ll 1$ and $Ha \gg 1$ as follows

$$D_M \cong 3\pi\eta_M d_P v_{m,B}\left[1+\frac{3}{8}Ha+\mathrm{O}(Ha^2)\right] \quad (Ha \ll 1) \tag{11}$$

$$D_M \cong 3\pi\eta_M d_P v_{m,B}\left[\frac{1}{3}Ha+\mathrm{O}(Ha^2)\right] \quad (Ha \gg 1) \tag{12}$$

where $Ha = B\frac{d_P}{2}(\frac{\sigma_M}{\eta_M})^{1/2}$ and σ_M is the electrical conductivity of liquid melt at a certain temperature and $v_{m,B}$ is the terminal particle velocity under the magnetic field.

For laminar flow, the terminal velocity of the particle can be derived via Stokes' law [25].

$$v_{m,B} \cong v_m \frac{1}{\left[1+\frac{3}{8}Ha+\mathrm{O}(Ha^2)\right]} \ (Ha \ll 1) \tag{13}$$

$$v_{m,B} \cong v_m \frac{1}{\left[\frac{1}{3}Ha+\mathrm{O}(Ha^2)\right]} \ (Ha \gg 1) \tag{14}$$

where $v_m = (\rho_P - \rho_M)gd_P^2/18\eta_M$.

In the middle range, there is no precisely analytical equation for D_M. Yasuda [8] derived an estimated equation for the case of $Ha \cong 1$ and the velocity is expressed as

$$v_{m,B} \cong v_m \frac{1+Ha}{1+\frac{11}{8}Ha+\frac{1}{3}Ha^2} \ (Ha \cong 1) \tag{15}$$

The set of the expressions is complicated to use and it is not evident to find a proper physical background [8]. To get simpler

expressions of the melt viscosity under a strong magnetic field, some mathematical process was conducted by fitting Equations (13) to (15). We found the following equation (Equation (16)) fits the whole Hartmann number range well and it is also easier to be understood physically according to [8] (Fig. 5). The viscosity of the melt after imposing a magnetic field can be obtained according to the Stokes' law and Equations (11) to (16). Therefore, in the following calculations, we adopted Equation (17) to evaluate the magnetic field effect on the melt viscosity (effective viscosity).

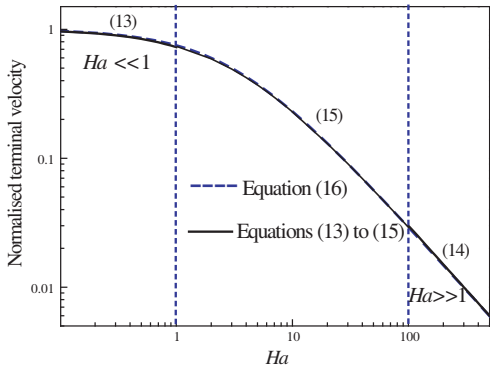

Figure 5. Comparison of the previous and present estimations for the normalised terminal velocity v.s. the Hartmann number.

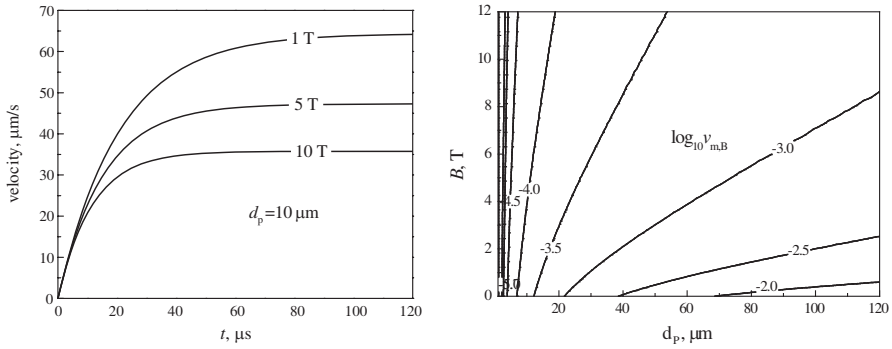

Figure 6. Effect of the magnetic field density on (a) the migration velocity for an alumina particle of 10 μm; (b) the maximum velocity with different particle size.

$$v_{m,B} \cong v_m \frac{1}{1+\frac{1}{3}Ha} \tag{16}$$

$$\eta_{M,B} \cong \eta_M \left(1+\frac{1}{3}Ha\right) \tag{17}$$

In the present case, the migration velocity of a spherical alumina particle can be calculated according to Equations (6) and (17)

$$v_P = \frac{d_P^2}{18\eta_{M,B}} \left[(\chi_M - \chi_P)\frac{1}{\mu_0} B_z \frac{dB_z}{dz} + (\rho_P - \rho_M)g\right]\left[1-\exp\left(-\frac{t}{\tau}\right)\right] \tag{18}$$

where $\tau = (\rho_P + 0.5\rho_M)d_P^2 \big/ 18\eta_{M,B}$ is the relaxation time.

Figure 6 gives the effect of the magnetic field density on the migration velocity of an alumina particle in a liquid aluminum at 933 K. The velocity reaches a maximum value in a very short time of around 40–100 µs and the time can be decreased by the magnetic field according to Equation (18) (Fig. 6(a)). Additionally, the maximum velocity will be reduced due to the increase of the magnetic field density. In Fig. 6(b), a clear hindering of the particle migration velocity presents when the magnetic field is high enough which can modify the velocity of pushed melt by the particle migration that cuts the magnetic lines (Fig. 3 and [14]). It will directly influence the interaction force induced by the particle migration according to Equation (10).

3.2. Effect of the Magnetic Field Density on the Particle-particle Interaction

To elucidate the strong magnetic effect on the feeble magnetic particle-particle interaction, the interaction forces were calculated by using Equations (7) to (10) and the theoretical model in [14]. As illustrated in Fig. 7, with the increase of the particle size, both the interparticle force due to the magnetisation (attractive force F_{12}) and the interparticle force due to the particle migration (repulsive force F') increase. But the repulsive force has smaller values than the attractive force when the particle size is smaller. However, it increases faster with the particle size, resulting in a critical diameter where the resultant magnetic interaction force becomes from attractive (positive values) into repulsive (negative values) as shown in Fig. 8. The white dashed line in Fig. 8 represents the change of the critical particle size with different magnetic field densities. It means that, in a conductive fluid, the strong magnetic field effect depends on the particle size, indicating a counteracting behavior and controlling the particle assembly morphologies. This is one of the reasons why the agglomeration of large particles in conductive fluid can be limited and

the particles repulse each other in a strong magnetic field and such phenomenon has been verified by recent experimental observations [7–11]. With the decrease of magnetic flux density, the magnitudes of the forces drop dramatically and become negligible compared with other forces, e.g., gravity force or convection [14]. This means that only under a magnetic field with high enough densities, Al_2O_3 particles become controllable by the magnetic field and those smaller than the critical size tend to be attracted to each other, while those larger than the critical size tend to be repelled.

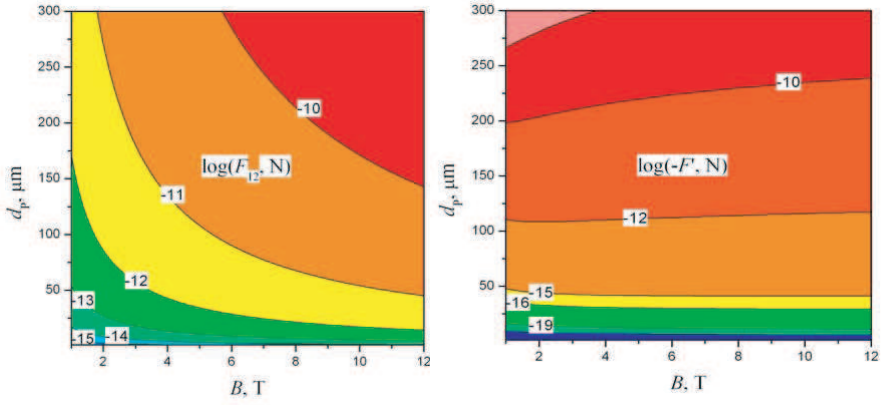

(a) (b)

Figure 7. Comparison of (a) the attractive force F_{12} and (b) the repulsive force F' under different magnetic fields.

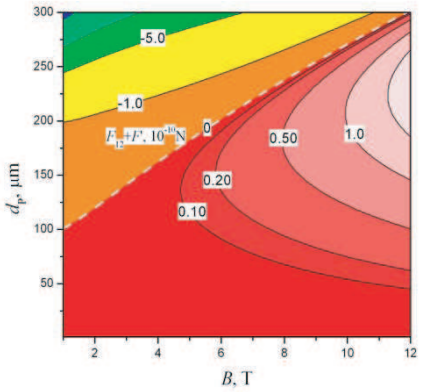

Figure 8. Effect of the magnetic flux density on the critical diameter.

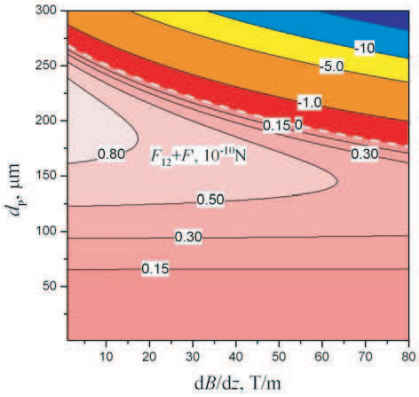

Figure 9. Effect of magnetic field gradient on the critical particle size.

3.3. Effect of the Magnetic Field Gradient on the Particle-particle Interaction

According to Equation (18), the particle velocity can be increased by the increase of magnetic field gradient product (BdB/dz). The interparticle force due to the fluid flow is directly related with the particle velocity $F' \propto v_P^2$ (Equation (10)). It indicates that the interaction behavior would be different under different gradient magnetic fields. A specific magnetic field gradient or gradient product can be obtained by adjusting the current in the superconducting coils of the magnet. Therefore, the dependence of the resultant interaction force ($F_{12} + F'$) on the magnetic field gradient product (BdB/dz) was investigated. As shown in Fig. 9, for two attached Al_2O_3 particles, the value of the resultant force decreases with the increase of the Faraday force (related with the magnetic field gradient, Equation (3)). It can be concluded that the interparticle repulsive force F' becomes more dominated when the particle migration is accelerated. Additionally, the critical particle size with an attractive-to-repulsive transition reduces at the same time as indicated by the white dashed line in Fig. 9. In a strong magnetic field, the magnetic field effect on micrometer sized non-magnetic particles becomes stronger with the increase of the magnetic field density [27]. However, their migration in a conductive fluid will be constrained due to the additional contribution to the fluid viscosity by the magnetic field (Equation (17)) according to Fig. 6. At the same time, the transition critical particle size is increased by increasing the magnetic field density (Fig. 8). During materials preparation, in most cases where we want to manipulate particles, the sizes should be as small as possible, e.g., sub-micrometer particles [28]. Therefore, the results from Fig. 9 can provide methods to control the separation of smaller particles by increasing the magnetic field gradient or by increasing the particle migrating velocity according to Equation (6). In practice, the critical particle size can be decreased by raising the conductive fluid velocity as well and a method related with non-magnetic particles (even in sub-micrometer sized) dispersion in a conductive fluid and/or assembly morphology controlling can be further proposed.

4. CONCLUSIONS

The magnetic interaction behaviors between two migrating non-magnetic particles and particle-fluid in a conductive fluid are analytically calculated and compared. The magnetic interaction forces become dominant only with a strong enough magnetic field. The counteracting behavior makes the particles controllable by adjusting

the external magnetic fields. In addition, by increasing the gradient product (BdB/dz) or the particle migrating velocity, the critical particle size for attractive-to-repulsive transition can be decreased. With a further understanding of this phenomenon we can not only explain the behavior of particle movement and interaction in strong magnetic field as reported in the literature, a method to non-magnetic particle manipulating using strong magnetic fields in materials preparation can also be provided.

ACKNOWLEDGMENT

Financial support from of the Flemish Institute for the Promotion of Scientific Technological Research in Industry (IWT) under contract SBO-PROMAG (60056) is gratefully acknowledged.

REFERENCES

1. Hill, R., V. Sedman, S. Allen, et al., "Alignment of aromatic peptide tubes in strong magnetic fields," *Advanced Materials*, Vol. 19, No. 24, 4474–4479, 2007.
2. Boamfa, M., S. Lazarenko, E. Vermolen, A. Kirilyuk, and T. Rasing, "Magnetic field alignment of liquid crystals for fast display applications," *Advanced Materials*, Vol. 17, No. 5, 610–614, 2005.
3. Butter, K., P. Bomans, P. M. Frederik, G. J. Vroege, and A. P. Philipse, "Direct observation of dipolar chains in iron ferrofluids by cryogenic electron microscopy," *Nature Materials*, Vol. 2, No. 2, 88–91, 2003.
4. Fang, W., Z. He, X. Xu, Z. Mao, and H. Shen, "Magnetic-field-induced chain-like assembly structures of Fe_3O_4 nanoparticles," *EPL*, Vol. 77, 68004, 2007.
5. Yellen, B., O. Hovorka, and G. Friedman, "Arranging matter by magnetic nanoparticle assemblers," *Proceedings of the National Academy of Sciences of the United States of America*, Vol. 102, No. 25, 8860–8864, 2005.
6. Yavuz, C. T., J. T. Mayo, W. W. Yu, et al., "Low-field magnetic separation of monodisperse Fe_3O_4 nanocrystals," *Science*, Vol. 314, 964–967, 2006.
7. Li, X., Z. Ren, and Y. Fautrelle, "Alignment behavior of the primary Al_3Ni phase in Al-Ni alloy under a high magnetic field," *Journal of Crystal Growth*, Vol. 310, No. 15, 3488–3497, 2008.

8. Yasuda, H., I. Ohnaka, O. Kawakami, K. Ueno, and K. Kishio, "Effect of magnetic field on solidification in Cu-Pb monotectic alloys," *ISIJ International*, Vol. 43, No. 6, 942–949, 2003.
9. Takayama, T., Y. Ikezoe, H. Uetake, N. Hirota, and K. Kitazawa, "Interactions among magnetic dipoles induced in feeble magnetic substances under high magnetic fields," *Physica B*, Vol. 346–347, 272–276, 2004.
10. Jin, F., Z. Ren, W. Ren, K. Deng, Y. Zhong, and J. Yu, "Effects of a high-gradient magnetic field on the migratory behavior of primary crystal silicon in hypereutectic Al-Si alloy," *Science and Technology of Advanced Materials*, Vol. 9, 024202, 2008.
11. Ren, Z., X. Li, Y. Sun, Y. Gao, K. Deng, and Y. Zhong, "Influence of high magnetic field on peritectic transformation during solidification of Bi-Mn alloy," *Calphad*, Vol. 30, No. 3, 277–285, 2006.
12. Iwai, K., J. Akiyama, M. Sung, I. Furuhashi, and S. Asai, "Application of a strong magnetic field on materials fabrication and experimental simulation," *Science and Technology of Advanced Materials*, Vol. 7, No. 4, 365–368, 2006.
13. Takayama, T., Y. Ikezoe, H. Uetake, N. Hirota, and K. Kitazawa, "Self-organization of nonmagnetic spheres by magnetic field," *Applied Physics Letters*, Vol. 86, No. 23, 234103–234103, 2005.
14. Sun, Z., T. Kokalj, M. Guo, F. Verhaeghe, O. Van der Biest, B. Blanpain, and K. Van Reusel, "Effect of the strong magnetic field on the magnetic interaction between two non-magnetic particles migrating in a conductive fluid," *EPL*, Vol. 85, 14002, 2009.
15. Sun, Z., M. Guo, T. Kokalj, O. Van der Biest, and B. Blanpain, "Migration and interaction behavior of electrical-insulating particles in a conductive melt under strong magnetic field with high gradient," *EPD Congress 2009, TMS 2009*, S. Howard, P. Anyalebechi, and L. Zhang (eds.), 785–792, San Francisco, CA, Feb. 15–19, 2009.
16. Ravaud, R. and G. Lemarquand, "Magnetic field in MRI yokeless devices: Analytical approach," *Progress In Electromagnetics Research*, PIER 94, 327–341, 2009.
17. Huang, H., Y. Fan, F. Kong, B.-I. Wu, and J. A. Kong, "Influence of external magnetic field on a symmetrical gyrotropic slab in terms of goos-hänchen shifts," *Progress In Electromagnetics Research*, PIER 82, 137–150, 2008.
18. Stuhler, J., A. Griesmaier, T. Koch, M. Fattori, T. Pfau, S. Giovanazzi, P. Pedri, and L. Santos, "Observation of dipole-

dipole interaction in a degenerate quantum gas," *Physical Review Letters*, Vol. 95, 150406, 2005.

19. Sharma, M., Govind, A. Pratap, et al., "Role of dipole-dipole interaction on the magnetic dynamics of anisotropic layered cuprate antiferromagnets," *Physica Status Solidi (B), Basic Research*, Vol. 226, No. 1, 193–202, 2001.
20. Totten, G. E. and D. Scott, *Handbook of Aluminum*, Marcel Dekker, Inc., New York, United States, 2003.
21. Weast, R. C., M. J. Astle, and W. H. Beyer, *CRC Handbook of Chemistry and Physics*, CRC Press, Inc., Florida, USA, 1983–1984.
22. Yamaguchi, M. and Y. Tanimoto, *Magneto-Science (Magnetic Field Effects on Materials: Fundamentals and Applications)*, Springer-Verlag Berlin Heidelberg, New York, 2006.
23. Sun, C., H. Geng, N. Zhang, X. Teng, and L. Ji, "Viscous feature of Sb-Bi alloy under magnetic field," *Materials Letters*, Vol. 62, No. 1, 73–76, 2008.
24. Ghauri, S. and M. Ansari, "Increase of water viscosity under the influence of magnetic field," *Journal of Applied Physics*, Vol. 100, No. 6, 066101–066102, 2006.
25. Chester, W., "The effect of a magnetic field on Stokes flow in a conducting fluid," *Journal of Fluid Mechanics*, Vol. 3, 304–308, 1957.
26. Sun, Z., M. Guo, J. Vleugels, O. Van der Biest, and B. Blanpain, "Numerical calculations on inclusion removal from liquid metals under strong magnetic fields," *Progress In Electromagnetics Research*, PIER 98, 359–373, 2009.
27. Asai, S., "Application of high magnetic fields in inorganic materials processing," *Modeling and Simulation in Materials Science and Engineering*, Vol. 12, 1–12, 2004.
28. Snezhko, A., I. Aranson, and W. Kwok, "Dynamic self-assembly of magnetic particles on the fluid interface: Surface-wave-mediated effective magnetic exchange," *Physical Review E*, Vol. 73, 041306, 2006.